Direct observation of the soft-mode dispersion in the incipient ferroelectric $KTaO_3$

Yuki Ichikawa,* Masaya Nagai, and Koichiro Tanaka†
Department of Physics, Graduate School of Science, Kyoto University, Sakyo-ku, Kyoto 606-8502, Japan
(Received 31 July 2004; revised manuscript received 16 December 2004; published 31 March 2005)

Far-infrared dispersion of the complex dielectric constant in incipient ferroelectric $KTaO_3$ has been revealed by terahertz time-domain spectroscopy (THz-TDS) in the temperature range from 8 K to 300 K. The real part of the complex dielectric constant in the far-infrared region is larger than the static permittivity. Through the analysis using a single Lorentz oscillator model, we conclude that the origin of the extremely large static permittivity in $KTaO_3$ and its anomalous behavior at low temperatures are almost fully attributed to the TO_1 mode dispersion and the suppression of the softening.

DOI: 10.1103/PhysRevB.71.092106 PACS number(s): 77.22.−d, 07.57.−c, 78.20.Ci, 78.47.+p

Incipient ferroelectric potassium tantalate ($KTaO_3$) has been of interest from the viewpoint of the quantum effect in the dielectric property. In $KTaO_3$, the dielectric permittivity increases with decreasing temperature, obeying the Curie-Weiss law. Even at low temperatures, it maintains a large dielectric constant without undergoing a ferroelectric phase transition.[1] A second-order phase transition can be induced by external stimuli, such as impurity doping,[2] electric field,[3] and pressure,[4] indicating that the novel dielectric property should come from the competition between the ferroelectric ordering and quantum fluctuation. In addition, $KTaO_3$ is the most suitable material for clarifying the nature of the quantum effect because $KTaO_3$ holds a simple cubic structure as low as 4 K.

Mode softening at the Brillouin zone center has been studied energetically by hyper-Raman scattering (HRS)[5] and by neutron scattering[6] to clarify the origin of the dielectric anomaly. Figure 1 shows temperature dependence of the permittivity in $KTaO_3$ estimated by several methods. Actually, the static permittivity derived from the TO_1 mode frequency[5] and the LO_1 mode frequency[7] (asterisks) with the Lyddane-Sachs-Teller (LST) relation shows good accordance with the permittivity measured at 100 Hz (triangles). This suggests that the origin of the dielectric anomaly should be attributed to suppression of the softening of the TO_1 mode by the quantum fluctuation. However, another possibility, namely, that relaxators with frequency below the soft-mode frequency cause the anomalous behaviors of the dielectric property at low temperature, was proposed. Maglione has reported[8] that relaxators of about 10 ns relaxation time appear below 65 K and lead to the large dielectric constant. In addition, other remarkable reports on the low-frequency excitation in the GHz region in $KTaO_3$ have been reported.[9,10]

In order to clarify the origin of the extremely large dielectric constant, it is crucial to measure the dielectric constant directly in the frequency region just below the TO_1 mode frequency. In this report, we evaluate the dielectric constant in a pure $KTaO_3$ crystal using terahertz time-domain spectroscopy (THz-TDS).[11] Since the amplitude attenuation and relative phase shift of a transmitted THz electric field are measured in this technique, optical constants can be directly evaluated without using Kramers-Kronig analysis. Thus a complex dielectric constant is expected to be more accurately determined than conventional FTIR techniques in the far-infrared region.[7,12]

A pure $KTaO_3$ crystal, grown by the spontaneous nucleation technique,[13] was cut into the size of $5\times5\times0.05$ mm^3 and polished using diamond slurry. A square plane sample with (100) surfaces was prepared. In order to ensure the quality of this sample, an ac impedance measurement was performed. The triangles in Fig. 1 show the temperature dependence of the dielectric constant at 100 Hz. The dielectric constant, 275 at room temperature, is increased to 4500 with temperature cooling down to 3 K, exhibiting critical behavior as mentioned above. These values are almost the same as those previously reported.[14]

In the THz-TDS system, a mode-locked Ti:sapphire laser beam (pulse duration of 70 fs, repetition 82 MHz, and center wavelength of 810 nm) was divided into two beams using a beam splitter. One beam was focused on a (100)-oriented InAs in 1 T magnetic field for the generation of a THz wave,[15] and the other was focused into a (110) ZnTe crystal with 1 mm thickness for the detection of the THz wave by electro-optic sampling (EO sampling). The emitted THz radiation was collimated and focused onto the sample with two off-axis parabolic mirrors. The sample was held in a conductive-type liquid helium cryostat at temperatures from

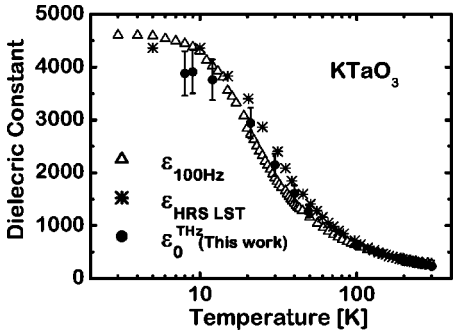

FIG. 1. The temperature dependence of the static dielectric constant. The triangles show dielectric constants measured at 100 Hz. The asterisks show those derived from the soft-mode frequencies obtained by hyper-Raman spectroscopy (Ref. 5) with the reported LO_1 mode frequency (Ref. 7) under the assumption of $\varepsilon_\infty=50$ using the LST relation. The closed circles show the static dielectric constants obtained from the dispersion in the THz region (this work).

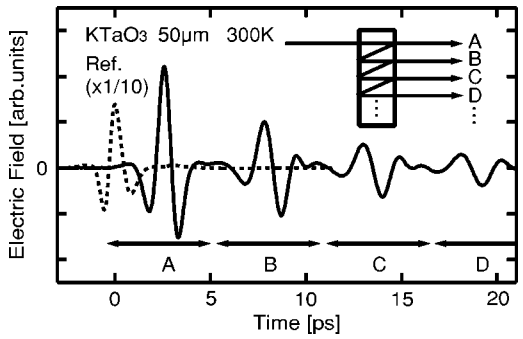

FIG. 2. Temporal waveform of the THz pulse after transmission of the $KTaO_3$ single crystal (thickness: 50 ± 2 μm). A is the primary pulse without any reflection. B, C, and D are due to the multiple internal reflection peaks in the sample. The dashed line indicates the temporal shape of the initial pulse measured without sample.

8 K to room temperature. The polarization of the THz wave was in parallel with the [100] direction of the sample. The transmitted THz wave was collected and focused on the ZnTe crystal with two parabolic mirrors. The birefringence of the sampling beam modulated by the electric field of the THz pulse was measured using a quarter wave plate, a polarization prism, and two balanced detectors. For phase-sensitive detection, the THz pulse was modulated by an acoustic-optic modulator operating at 80 kHz. The detectable spectral range in this system was from 0.2 to 2.5 THz with a sensitivity of S/N 3000 in the electric field amplitude.

Figure 2 shows a typical temporal waveform of the transmitted THz electric field through a $KTaO_3$ crystal at 300 K. We take the origin of the time scale at the peak position of the reference pulse, which is measured without the sample and shown by a dashed line. A pulse sequence with regular intervals, denoted as shown in Fig. 2, can be observed. The arrival of the first pulse was significantly delayed by 2.6 ps to the reference pulse. From this retardation and the sample thickness (50 ± 2 μm), we can roughly estimate the dielectric constant of the sample. With the assumption of $n \gg \kappa$, defining the complex refractive index $\tilde{n}=n+i\kappa$, the real part of the dielectric constant is obtained as 276 ± 20, which is in good accordance with the permittivity at 100 Hz (275) by the ac impedance measurement at room temperature. The subsequent pulses, B, C, and D, are attributed to the signals from multiple internal reflections inside the sample (inset of Fig. 2).

Figure 3 shows the waveforms of the transmitted THz wave at several temperatures. Only the first pulse is presented. The top curve is the temporal profile of the reference pulse on a scale of 1/10. At 300 K, the transmitted THz waveform has a similar shape to the reference waveform. With decreasing temperature, the amplitude of the signal is significantly attenuated. The attenuation of the pulse represents an enhancement of the reflection and/or absorption in the sample. The closed circles in Fig. 3 indicate the first peak positions. The pulse is extensively delayed at low temperatures. This temperature dependence of the retardation indicates that the real part of the dielectric constant, strictly speaking, the index of refraction, is increased with decreasing temperature. The dielectric constant is roughly estimated

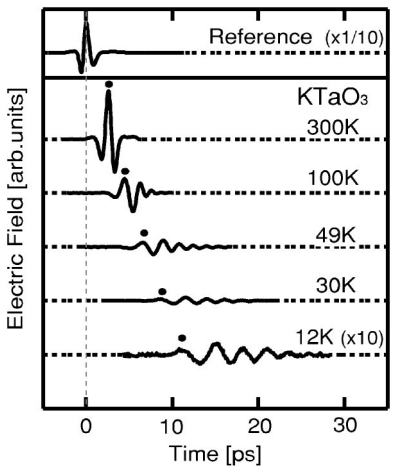

FIG. 3. The waveforms of THz pulses transmitted through the sample at several temperatures. A temporal profile without samples is shown at the top for the reference on a scale of 1/10. Dots indicate the positions of the first positive peaks.

as 4490 ± 420 at 12 K. As for the pulse shape, the transmitted pulse width becomes broad and its periodic structure becomes extended with decreasing temperature. Qualitatively, the pulse broadening means the narrowing of the spectrum, suggesting that the incident THz pulse loses its high-frequency part of the spectrum during the propagation in the sample. The loss should come from the softening of the TO_1 mode at low temperatures.

For accurate estimation of the dielectric properties, we evaluated dielectric function $\tilde{\varepsilon}(\omega)$ from temporal profile of THz wave.[11] The pulse passing through two interfaces and traversing the sample, denoted as optical path "A" in Fig. 2, gives the transmitted electric field Fourier component $\tilde{E}_t(\omega)$ that is expressed as

$$\tilde{E}_t(\omega)=\tilde{t}_{vs}(\omega)\exp\left(i\frac{\sqrt{\tilde{\varepsilon}(\omega)}\omega d}{c}\right)\tilde{t}_{sv}(\omega)\tilde{E}_0(\omega), \qquad (1)$$

where $\tilde{E}_0(\omega)$ is the incident electric field, d is the thickness of the sample, c is the velocity of light in vacuum. $\tilde{t}_{vs}(\omega)=2/[\sqrt{\tilde{\varepsilon}(\omega)}+1]$, and $\tilde{t}_{sv}(\omega)=2\sqrt{\tilde{\varepsilon}(\omega)}/[\sqrt{\tilde{\varepsilon}(\omega)}+1]$ are Fresnel coefficients at the first and the second boundaries, respectively. Since $\tilde{E}_0(\omega)$ can be calculated from the reference pulse without the sample $\tilde{E}_{ref}(\omega)=\tilde{E}_0(\omega)\exp(i\omega d/c)$, $\tilde{\varepsilon}(\omega)$ can be numerically obtained from $\tilde{E}_t(\omega)$ and $\tilde{E}_{ref}(\omega)$ without any assumption.

Figure 4 shows the real (a) and imaginary (b) parts of the complex dielectric constant at several temperatures by solid curves. It is clear that the real part is larger than the permittivity obtained by the ac impedance measurement (Fig. 1). Both the real and imaginary parts of $\tilde{\varepsilon}$ exhibit frequency dispersions in which the magnitude increases in the high-frequency region, indicating that a resonant oscillator should exist in the higher-frequency region. The slope of the dispersion becomes steep with decreasing temperature, from which we anticipate a softening of the oscillator. The most probable

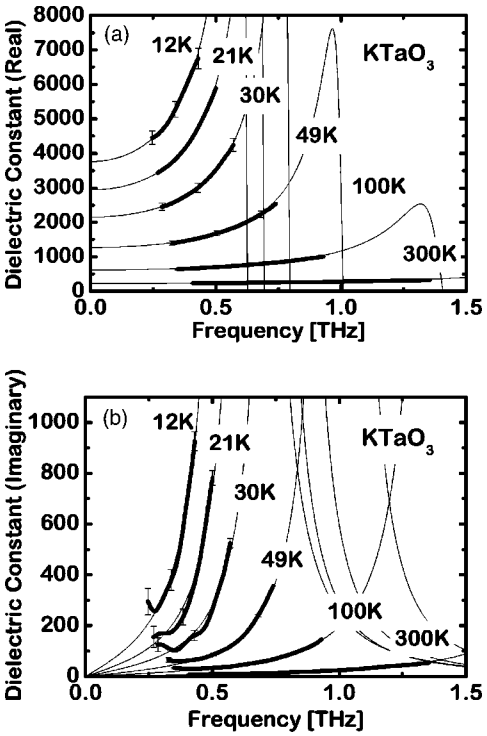

FIG. 4. The frequency dispersion of the real part (a) and the imaginary part (b) of complex dielectric constants at several temperatures. Bold lines are experimental results obtained by THz-TDS. Thin lines are dispersions calculated with a single Lorentz oscillator model.

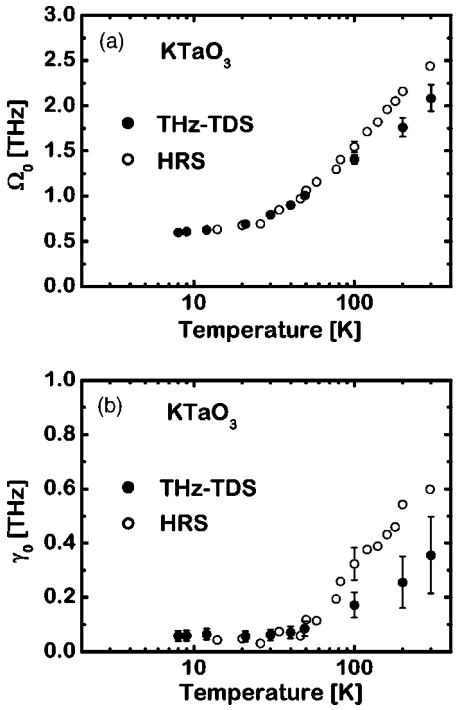

FIG. 5. The temperature dependence of the TO_1 mode frequency (a) and damping constant (b). The closed circles are the best-fitted parameters in a Lorentz oscillator model. The open circles are the reported values of hyper-Raman spectroscopy (Ref. 5).

candidate for the resonant oscillator is the TO_1 mode, the so-called "ferroelectric soft mode."

At this point, the frequency resolution should be discussed because the analysis of the first nonreflected signal brings about a restriction in the time domain. Since the interval of the internal reflection depends strongly on the temperature, the frequency resolution varies from 0.04 THz at 8 K to 0.11 THz at 300 K. Fortunately, this frequency resolution is good enough at each temperature to determine the dispersion curve.

We analyzed the dispersion of the dielectric constant in the THz region using a single Lorentz oscillator model. In the single Lorentz oscillator model, the complex dielectric constant can be expressed as

$$\tilde{\varepsilon}(\omega) = \varepsilon_\infty + \frac{(\varepsilon_0 - \varepsilon_\infty)\Omega_0^2}{\Omega_0^2 - \omega^2 - i\omega\gamma_0}, \tag{2}$$

where Ω_0 and γ_0 are the mode frequency and damping, respectively. ε_0 and ε_∞ are the low- and high-frequency limits of the relative complex dielectric constant, respectively. Note that ε_0 should be examined with the static dielectric constant measured by the ac impedance. Assuming $\varepsilon_\infty = 50$,[16] we estimated the best set of $(\Omega_0, \gamma_0, \varepsilon_0)$ by careful search of the least square value for the complex dielectric function. The parameters are determined with good accuracy by the least square analysis using the real and imaginary parts of the dielectric constant simultaneously. The thin lines in Fig. 4 show the fitted dispersions, which successfully reproduced the exprimental data in the lower frequency region than Ω_0.

The parameters of Ω_0, γ_0, and ε_0 are summarized by closed circles in Figs. 5(a), 5(b), and 1, respectively. We obtained $\Omega_0 = 2.09 \pm 0.15$ THz and $\gamma_0 = 0.35 \pm 0.14$ THz at 300 K. As temperature decreased, Ω_0 and γ_0 decreased to $\Omega_0 = 0.60 \pm 0.02$ and $\gamma_0 = 0.06 \pm 0.02$ THz at 8 K. The open circles in Figs. 5(a) and 5(b) are Ω_0 and γ_0 obtained by hyper-Raman scattering experiments.[5] Ω_0 determined by THz-TDS is almost in good agreement with the frequency parameters of the TO_1 mode obtained by hyper Raman scattering at low temperatures. γ_0 is also in good agreement with the hyper-Raman below 100 K, but an apparent deviation is observed above 100 K. These results prove that dispersions come from the TO_1 soft mode, at least below 100 K. The determined ε_0^{THz}, that is, the static dielectric constant extrapolated from the obtained dispersion, is identical with the temperature dependence of ε measured at 100 Hz (triangles in Fig. 1) with a reliability of 10%. This result means that the large permittivity of $KTaO_3$ is almost given by the dispersion of the TO_1 mode. The anomalous dielectric behavior at low temperatures is exclusively caused by the suppression of the TO_1 mode softening. As described above, the damping constant obtained by THz-TDS exhibits, qualitatively, a similar behavior to that of the hyper-Raman report,[5] decreasing linearly with decreasing temperature and being horizontal at low temperatures. This feature is also seen in that of $SrTiO_3$.[17] Such a behavior of the damping constant might be due to the anharmonic coupling with other phonons. The reason is unknown at the moment, but this phenomenon might be specific to quantum paraelectric materials. The obtained mode frequency slightly deviates from HRS above

100 K. One of the possible reasons is that the analysis with a single Lorentz oscillator model may be insufficient to reproduce the obtained dispersion at high temperatures. Actually, we neglected the contributions of other higher-frequency phonons to the dispersion and fixed $\varepsilon_\infty = 50$. The effect of the TO_2 mode (6.03 THz) should be taken into account in the analysis when the damping of the TO_2 mode becomes large and the TO_1 mode shifts away from the observable range at high temperatures. The present analysis disregarding the TO_2 mode dispersion may bring about the deviation of Ω_0 and γ_0 at high temperatures. However, it should be emphsized that, even in this case, such an effect of the background dielectric constant does not produce significant change of ε_0^{THz}. Possibly, the framework of a single Lorentz oscillator model itself might break down when anharmonicity of the TO_1 mode coming from the mode coupling gives a significant effect. Further measurements in the wide frequency region are required to reveal the whole profile of the soft mode dispersion and the anharmonicity.

In conclusion, we have performed THz-TDS on incipient ferroelectric $KTaO_3$ and determined the dispersion of the dielectric constant in the THz region, the frequency region just below the phonon energy. As a result, we observed the resonance of the TO_1 mode and its mode softening. The dispersion revealed by THz-TDS clearly shows that the soft mode yields the large static permittivity of $KTaO_3$. Almost all parts of the anomalous increase of the static permittivity appear to originate from the suppression of the softening of the TO_1 mode.

ACKNOWLEDGMENTS

This work was supported by the Grant-in-Aid for the 21st Century COE "Center for Diversity and Universality in Physics" from the Ministry of Education, Culture, Sports, Science, and Technology (MEXT) and was also financially supported by Strategic Information and Communications R&D Promotion Programme (SCOPE) from the Ministry of Public Management, Home Affairs, Posts, and Telecommunications, Japan.

*Electronic address: ichikawa.yuki@scphys.kyoto-u.ac.jp
†Also at Core Research for Evolutional Science and Technology (CREST), Japan Science and Technology Corporation, Japan.

[1] J. H. Barrett, Phys. Rev. **86**, 118 (1952).
[2] D. Rytz, U. T. Höchli, and H. Bilz, Phys. Rev. B **22**, 359 (1980).
[3] I. M. Buzin, I. V. Ivanov, N. N. Moiseev, and V. F. Chuprakov, Sov. Phys. Solid State **22**, 1200 (1980).
[4] H. Uwe and T. Sakudo, J. Phys. Soc. Jpn. **38**, 183 (1975).
[5] H. Vogt, Phys. Rev. B **51**, 8046 (1995).
[6] G. Shirane, Rev. Mod. Phys. **46**, 437 (1974).
[7] C. H. Perry and N. E. Tornberg, Phys. Rev. **183**, 595 (1969).
[8] M. Maglione, S. Rod, and U. T. Höchli, Europhys. Lett. **4**, 631 (1987).
[9] I. Katayama, M. Shirai, and K. Tanaka, J. Lumin. **102–103**, 54 (2003).
[10] E. Courtens, B. Hehlen, G. Coddens, and B. Hennion, Physica B **219&220**, 577 (1996).
[11] M. C. Nuss and J. Orenstein, in *Millimeter and Submillimeter Wave Spectroscopy of Solids*, edited by G. Grüner (Springer-Verlag, Berlin, 1998).
[12] K. F. Pai, T. J. Parker, and R. P. Lowndes, J. Opt. Soc. Am. **68**, 1322 (1978).
[13] D. M. Hannon, Phys. Rev. **164**, 366 (1967).
[14] S. H. Wemple, Phys. Rev. **137**, A1575 (1965).
[15] N. Sarukura, H. Ohtake, S. Izumida, and Z. Liu, J. Appl. Phys. **84**, 654 (1998).
[16] We assume the parameter of $\varepsilon_\infty = 50$, estimated from ε_0 at 100 Hz, and the early reported frequencies of the TO_1 mode [5] and LO_1 mode (5.58 THz) [7], using the LST relation. From the least-square analyses using different values of ε_∞, we conclude that this value is reasonable in the framework of a single Lorentz oscillator model.
[17] A. Yamanaka, M. Kataoka, Y. Inaba, K. Inoue, B. Hehlen, and E. Courtens, Europhys. Lett. **50**, 688 (2000).